JOURNAL OF GEOPHYSICAL RESEARCH, VOL. 106, NO. 12, PAGES 30755–30769, DECEMBER 10, 2001

Regional electrical resistivity structure of the southern Canadian Cordillera and its physical interpretation

Juanjo Ledo and Alan G. Jones
Geological Survey of Canada, Ottawa, Ontario, Canada

Abstract. The regional geoelectric crustal structure of the southern and central Canadian Cordillera of western Canada is interpreted from the inversion of magnetotelluric data along five profiles crossing the physiographic morphogeological belts, with emphasis on the Intermontane and Omineca Belts. Decomposition of the tensor impedance response estimates demonstrates that large-scale regional structures can be reasonably approximated along each profile as two-dimensional, with dominant geoelectric strikes of either $-30°$ or $+15°$, depending on profile location. These profile-specific strike directions are consistent with a local clockwise rotation of crustal structures in the southern Intermontane and Omineca Belts suggested by others based on paleomagnetic data and palinspastic reconstructions. Comparing the resistivity models derived from two-dimensional inversions of the distortion-corrected data along each profile allows us to construct an orogen-scale three-dimensional resistivity model for southern British Columbia. Generally, the model shows a resistive upper crust overlying a conductive lower crust. The resistivity of the lower crust beneath the Intermontane Belt is independent of latitude and is similar for all profiles. In stark contrast, a 2 orders of magnitude variation in lower crustal resistivity is observed along strike in the Omineca Belt, with higher conductivities to the south in the region of Eocene extension and lower conductivities to the north in the unextended part of the belt. Such spatial association has noteworthy implications for the cause of lower crustal resistivity in active, or recently active, young regions. Our preferred interpretation of the observed lower crustal resistivities with other geophysical data is in terms of fluids, with brines dominating for the most part but partial melt possible at the base of the crust in specific localities. We attribute the along-strike variation in the Omineca Belt mostly to variation in fluid content and interconnectivity, with the lowermost crust of the southern Omineca Belt being partially molten. This physical state difference is a consequence of degree of extension and implies that mantle-derived fluids are important for lower crustal resistivity.

1. Introduction

The Cordillera of western North America comprises a region of oceanic and island arc terranes accreted to North America since the Neoproterozoic, with most of this westward growth occurring during the last 200 Myr. It is within this geological mosaic that the concept of terranes was first articulated [*Coney et al.*, 1980], and this concept has been successfully applied worldwide. During the decade 1985–1995, there was extensive acquisition of geological and geophysical data in southern British Columbia (BC) as part of the Canadian multidisciplinary Lithoprobe program of study of the southern Canadian Cordillera [*Gabrielse and Yorath*, 1991; *Clowes et al.*, 1992; *Cook*, 1995, and references therein]. The principal results from the Lithoprobe southern Canadian Cordillera studies have already appeared [*Cook*, 1995], but there remain intriguing questions and new ones posed by compilations and reexaminations of the data. The question raised by such a compilation and reexamination "What is the state of the lower crust beneath the Intermontane and Omineca belts?" is discussed here.

From 1985 to 1990, magnetotelluric (MT) data were acquired at over 450 sites in southern BC as part of Lithoprobe activities. Quantitative interpretations have been presented by a number of different authors, focusing on regional structures and on several specific geological targets [*Kurtz et al.*, 1990; *Majorowicz and Gough*, 1991, 1994; *Jones and Dumas*, 1993; *Jones et al.*, 1992a, 1992b, 1993; *Gupta and Jones*, 1995; *Marquis et al.*, 1995]. *Jones and Gough* [1995] compiled all available MT data, including data acquired in the early 1980s as part of the Canadian Geothermal Energy Program, and provided a qualitative interpretation of the complete data set. However, a quantitative interpretation of all data, after analysis and modeling using a consistent methodology, has not previously been accomplished. The main purpose of this paper is to model the electrical resistivity distribution of the southern Canadian Cordillera at orogen scale with specific emphasis on the Intermontane and Omineca Belts. We apply a consistent analysis and inversion approach to all data, thereby ensuring that differences between profiles can be attributed mainly to differences in rock properties, not to differences in methodologies. We use MT tensor decomposition techniques developed over the last decade to identify and remove distortions caused by local near-surface features, and we derive the regional two-dimensional (2-D) MT impedances in the most appropriate geoelectric strike directions. We then invert these regional impedances to derive 2-D resistivity models valid for subsets of the different profiles. The resulting resistivity models are compared with other geophysical and geological data and inferences drawn about the physical state and fluid content of the lower crust.

Previous studies were all consistent in revealing a lower crust with low electrical resistivity. Here we examine the lower crustal resistivity in more detail and provide an explanation for its variation between and within the central two morphogeological belts. We tie this explanation to a localized Eocene extension event

Paper number 2001JB000358.
0148-0227/01/2001JB000358$09.00

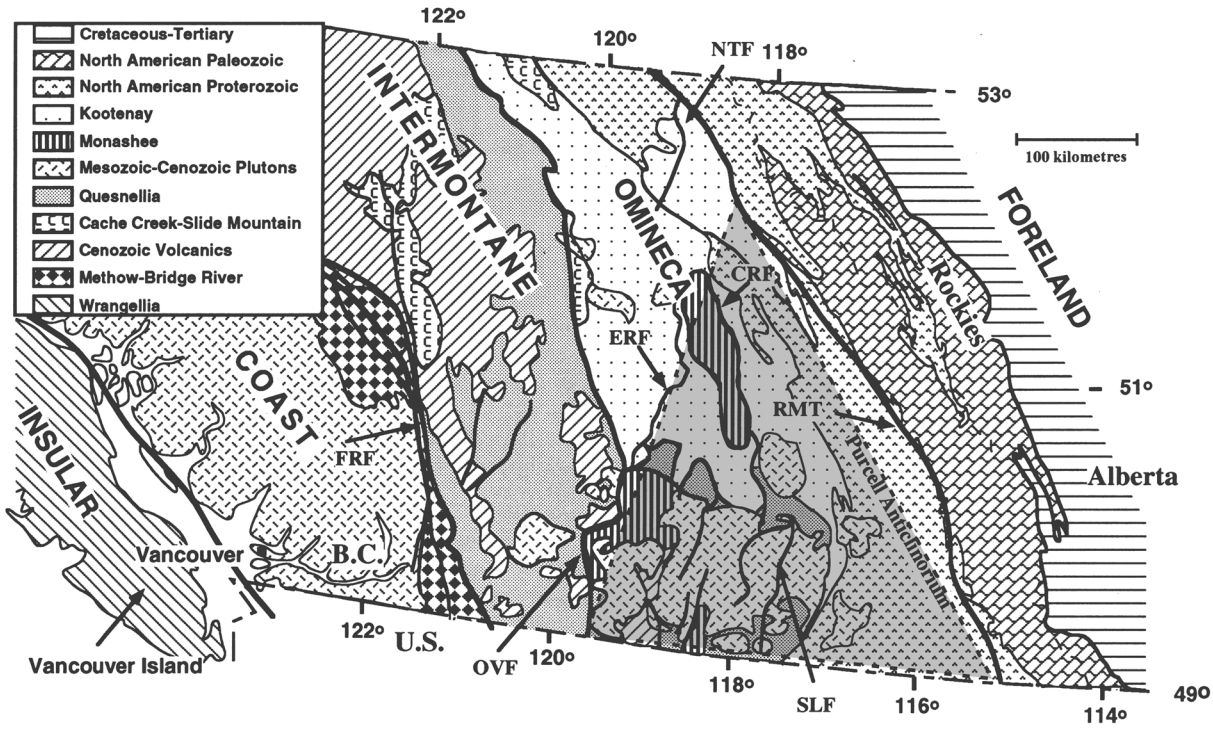

Figure 1. Regional geology and morphogeological belts of the southern Canadian Cordillera. CRF, Columbia River Fault; ERF, Eagle River Fault; FRF, Fraser River Fault; NTF, North Thompson Fault; OVF, Okanagan Valley Fault; RMT, Rocky Mountain Trench; SLF, Slocan Lake Fault. Shaded area is zone of early Eocene extension in the Omineca Belt. Modified from *Nesbitt and Muehlenbachs* [1995].

and conclude that mantle-derived fluids contribute to decreasing lower crustal resistivity.

2. Morphogeological Belts and Eocene Extension in the Southern Omineca

Morphogeologically and physiographically, the southern half of the Canadian Cordillera is divided into five major belts (Figure 1) broadly representing fault zone bounded geological units of regional extent. With the exception of the Foreland Belt, each belt comprises a collage of predominantly allochthonous terranes, and each terrane is characterized by its own geological and tectonic history different from its neighbors. From east to west these belts are named the Foreland Belt, the Omineca Belt, the Intermontane Belt, the Coast Belt, and the Insular Belt, and their development reflects Mesozoic and Cenozoic collision and deformation along the northwestern margin of North America. The following brief description of each belt is based on the work by *Gabrielse and Yorath* [1991].

The Foreland Belt contains rocks mainly deposited from latest Proterozoic to late Jurassic times along the long-lived rifted passive margin of western ancestral North America, together with late Mesozoic synorogenic clastics. The Omineca Belt is composed of highly compressed crystalline rocks that may represent the relic roots of Andean-type mountains uplifted behind a subduction zone active in late Mesozoic time. The central belt, the Intermontane Belt, is more subdued physiographically than its two flanking belts and consists of upper Paleozoic to mid-Mesozoic marine volcano-sedimentary sequences overlain by Cretaceous and Tertiary nonmarine sequences. The Coast Belt is made up of late Jurassic to early Tertiary rocks and is considered to contain the suture resulting from the mid-Cretaceous collision between the Insular Belt and the previously accreted Intermontane Belt. The outboard Insular Belt locally comprises latest Proterozoic to Paleozoic to Neogene volcanic and sedimentary rocks and subordinate granitic rocks added to the continent since 165 Ma. The accretion of intraoceanic terranes to an ancient continental margin is a process by which new continental crust was formed. However, taking into account the considerable volume of terranes accreted and the amount of juvenile crust formed, it appears that the dominant process is crustal recycling rather than crustal growth [*Monger*, 1993].

The geological record of relatively short-lived early to middle Eocene extension in southeastern British Columbia is observable within a pie-shaped segment shown in Figure 1. The extension is recorded to the south, near latitude 49°N, in rocks from the eastern Intermontane Belt across the Omineca Belt to the western Foreland Belt and extends northward to Mica Dam in the southern Rocky Mountain Trench at latitude 52.5°N [*Monger et al.*, 1994, and references therein]. This extension occurred between 59 Ma and 46 Ma [*Parrish et al.*, 1988], and the amount of extension at a latitude of 49.5°N (Penticton) was assessed at 80% [*Parrish et al.*, 1988] to 52% [*Bardoux and Mareschal*, 1994]. Farther north at 51°N (Revelstoke) the extension decreases to no more than 30% [*Brown and Journeay*, 1987]. Extension on mappable faults is not observed northward of 52°N (location of the Mica Dam (R. L. Brown, personal communication, 1995)). Most of this extension was accommodated on normal fault systems which bound exposed metamorphic core complexes, with east dipping faults mainly active between 58 and 52 Ma and west dipping faults active between 52 and 45 Ma [*Parrish et al.*, 1988].

During this extension, mantle-sourced Coryell Suite syenites were erupted and are presently exposed in the southernmost part of the Omineca Belt, with their most northerly exposure south of 50°N. The Coryell plutons have been dated at late early to middle

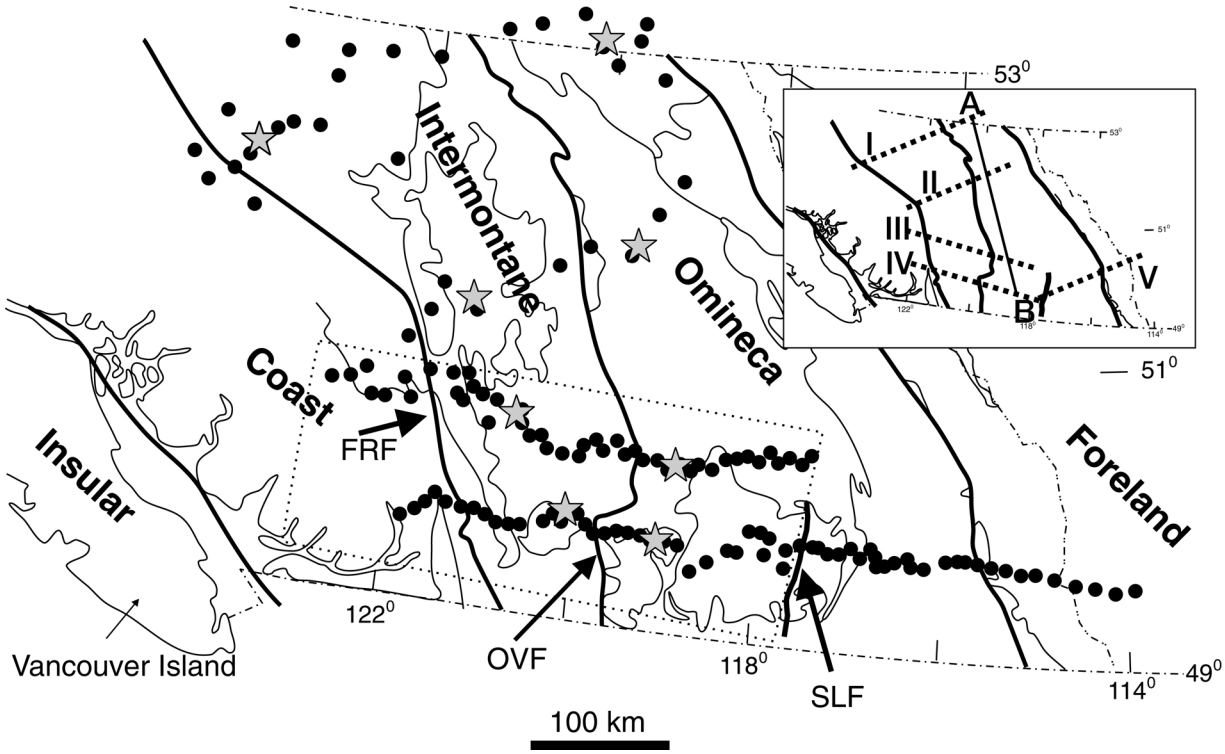

Figure 2. Map location of the MT sites (solid circles and stars) used in this paper over the morphogeological belts. FRF, Fraser River Fault; OVF, Okanagan Valley Fault; SLF, Slocan Lake Fault. Inset shows locations of the five profiles (dashed lines); the sites have been assigned to line A-B, trace of the along-strike crustal conductivity cartoon for the Omineca Belt presented in Figure 7. The apparent resistivity data from the sites marked as stars are compared against the model responses in Figure 6.

Eocene (51.1 ± 0.5 Ma [*Carr and Parkinson*, 1989]). Note that these intrusives do not extend as far north as Mica Dam but are limited to the southernmost Omineca Belt. We take these syenites as evidence for substantial mantle-derived magmatism at that time.

The cause of extension is contentious [see, e.g., *Bardoux and Mareschal*, 1994], but its timing is approximately coeval with the well-documented loss of Cordilleran mantle lithosphere at about 60 Ma. The overthickening of the crust and upper mantle may have led to gravitational collapse and subsequent "passive" detachment of the mantle lithosphere [*Coney and Harms*, 1984; *Ranalli et al.*, 1989; *Monger et al.*, 1994]. Otherwise, the change in relative plate motions at 56 Ma, which caused the Kula plate dextral transpression to become dextral transtension [*Engebretson et al.*, 1984], possibly aided, or even initiated, the extension and subsequent thinning of the lithosphere. Alternatively, the mantle lithosphere may have been lost due to "active" upwelling of asthenosphere caused by mantle convection, such as the continent overriding a spreading center [e.g., *Gough*, 1986; *Wilson*, 1991]. *Sonder and Jones* [1999] demonstrated the inability of any of these mechanisms individually to explain all the extensional deformation observed in the Basin and Range (western United States). Their arguments may also apply for the Omineca Belt extension, and a combination of mechanisms could have occurred. Whichever mechanisms are responsible, modeling suggests that rapid removal of the mantle lithosphere will quickly heat the remaining lithosphere and promote extension [*Mareschal*, 1994].

3. Regional Structural Geometry From Seismic Information

The most complete regional geophysical information for the southern Canadian Cordillera comes from reflection and refraction seismic profiling. The depth to Moho beneath the Foreland Belt is both imaged by reflection seismics and modeled from refraction seismics at ∼42 km and is shallower to the west by ∼10 km. This crustal thinning occurs abruptly at the easterly downdip location of the crustal-penetrating Eocene extensional Slocan Lake fault in the southern Omineca Belt [*Cook et al.*, 1992; *Zelt and White*, 1995].

In the Omineca and Intermontane Belts the seismic reflection data image three large crustal antiforms, the Monashee Complex, the Vernon antiform, and the central Nicola horst [*Cook*, 1995]. Below these structures the lower crust is interpreted to be a thin tapering wedge of modified North American cratonic basement extending westward to the Fraser River Fault. The interpreted Moho beneath these belts is imaged as a flat boundary, at ∼32 km depth, in sharp contrast to the high structural relief observed on the surface. In southeastern British Columbia the boundary between the Intermontane and Coast Belts is marked by the strike-slip Fraser River Fault that penetrates the entire crust [*Jones et al.*, 1992b].

4. Magnetotelluric Data and Regional Impedance Determination

The magnetotelluric method involves measuring the temporal fluctuations of the horizontal components of the natural electromagnetic field on the surface to determine the lateral and vertical variations of electrical resistivity of the Earth's interior [*Vozoff*, 1991; *Jones*, 1992]. The sensing distance is a function of the electrical resistivity of the Earth (ρ) and the period (T) of investigation. A reasonable measure of inductive scale length is given by the skin depth ($\delta \cong 500(\rho T)^{1/2}$ in meters, with T in

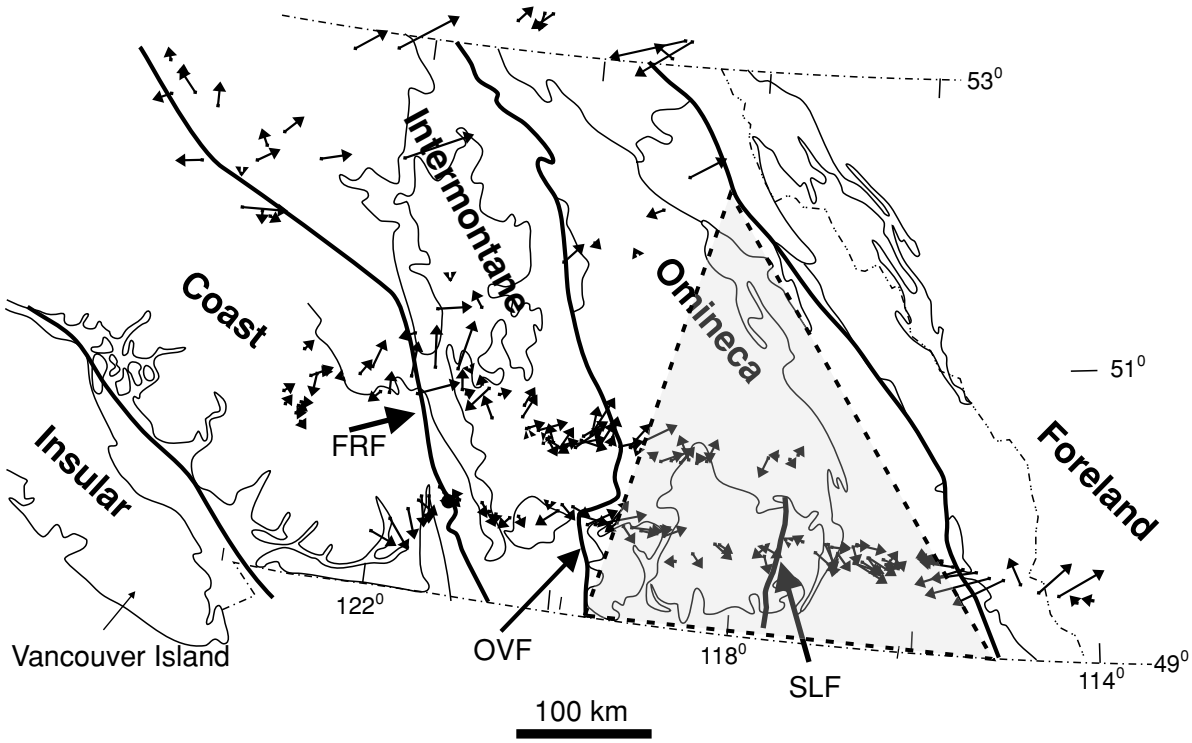

Figure 3. Real (reversed) induction vectors at a period of 64 s. Shaded area is zone of early Eocene extension in the Omineca Belt. Induction vector unit is 100 km.

seconds and ρ in Ω m), which is the depth by which incident electromagnetic (EM) fields have attenuated to $1/e$ of the surface value in a uniform half-space. Structures located farther away than a skin depth will have little influence on the observable EM fields.

Values of electrical resistivity of Earth materials in the crust and mantle are usually dominated by the presence of a minor constituent in the host rock matrix and are thus complementary to bulk property physical parameters determined by seismic and potential field methods. The electrical resistivity of a rock depends not only on the amount of ionic and/or electronic conductors present but also on their interconnection and geometric distribution within the host rock [*ELEKTB Group*, 1997]. The magnetotelluric method has proven successful at detecting zones of low electrical resistivity due to partial melting and/or fluids (ionic conduction [e.g., *Wannamaker et al.*, 1989; *Kurtz et al.*, 1990; *Jones and Dumas*, 1993; *Ledo et al.*, 2000; *Partzsch et al.*, 2000; *Wannamaker*, 2000]) and solid conductive phases, i.e., graphite and sulfides (electronic conduction [e.g., *Duba et al.*, 1994; *Cook and Jones*, 1995; *Gupta and Jones*, 1995; *Jones et al.*, 1997]). Such anomalies are often structurally or tectonically controlled, and thus MT is a useful technique for imaging tectonic and geodynamic processes that are difficult to sense remotely by other techniques [*Jones*, 1993].

MT data were acquired in the southern Canadian Cordillera during a number of surveys since 1980 (see *Jones and Gough* [1995] for a review). The majority of the data were recorded as part of the Lithoprobe program [*Clowes et al.*, 1992] along two east-west transects (profiles III, IV, and V in Figure 2 inset) between latitudes of 49°N and 51°N. The observational period range of these data is 0.002–1820 s, which allows us to image conductive structures from the near surface to the deep crust and uppermost mantle. *Majorowicz and Gough* [1991] recorded a second set of data along two NE-SW profiles (I and II in Figure 2 inset) using equipment with a smaller observational period range, 0.006–80.5 s, which limits resolution to predominantly midcrustal depths. A complete description of all available MT data and their characteristics is given by *Jones and Gough* [1995]. The locations of the subset of sites used in this work are shown in relation to the morphogeological belts in Figure 2. Figure 3 shows the (reversed) real induction vectors at 64 s. The vectors point toward anomalies located at midcrustal to lower-crustal depths. Sixty-four seconds is the longest period for what there are estimates from the majority of sites. Some authors have interpreted the induction vectors together with MT responses to study local features [i.e., *Gupta and Jones*, 1995; *Ritter and Ritter*, 1997]. In our case, typical errors associated with these vectors are almost as large as the vectors themselves; the poor quality of these vectors mitigate using them in quantitative analysis.

For elongated structures that have the horizontal scale length larger than the inductive scale length (at that particular period), electromagnetic induction separates into two modes. One mode is descriptive of the responses for electric currents flowing along the structure (transverse electric mode, or TE mode), and the other is for currents flowing across the structure (transverse magnetic mode, or TM mode). To estimate the regional 2-D TE and TM responses from the derived impedance tensor responses estimates, we applied *McNeice and Jones* [2001] multisite, multifrequency MT tensor decomposition code. The code is based on the galvanic distortion decomposition of *Groom and Bailey* [1989] and detects and partially removes the effects caused by local near-surface inhomogeneities. A parameter obtained from these analyses is the regional 2-D geoelectric strike at each site and its variation with increasing period, which is a proxy for increasing depth [see, e.g., *Marquis et al.*, 1995]. In addition, one derives a measure of the minimum structural dimensionality inherent in the data over the depth range of investigation.

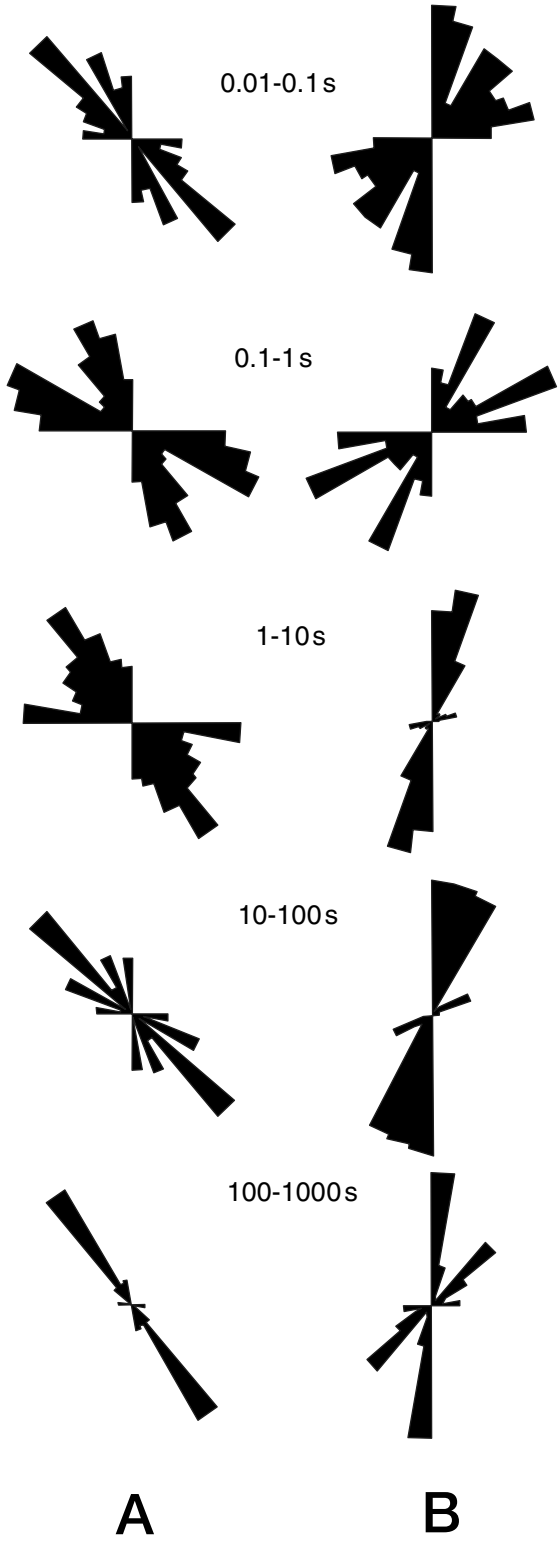

Figure 4. Rose diagrams giving the variation of the best fit for the regional azimuth to the *Groom and Bailey* [1989] galvanic distortion decomposition model for five different period bands between 0.01 and 1000 s. (a) Data from sites on profiles I, II, and V. (b) Data from sites on profiles III and IV.

After individual site-by-site decomposition of the data the sites were assigned to two different sets depending on the strike angle obtained for periods longer than 1 s (medium to large-scale structures). The sites located south of latitude 51°N and west of 117°W (rectangle in Figure 2) were assigned to one group, and the rest of sites were assigned to a second group. Figure 4 displays the strike directions as rose diagrams determined from the data at each site for both groups in the period range 0.01–1000 s in five decade-wide period bands. The individual site estimates of strike are weighted by the error of misfit to the *Groom and Bailey* [1989] (GB) distortion model, so the sites that cannot be fit to the GB distortion model were not considered in the rose diagram. For $T < 1$ s, there is no preferred geoelectric strike, as is evident from the azimuthal spread of the strike estimates. This lack of consistent strike is due to the presence of "local" features, i.e., upper crustal 3-D heterogeneity, on a scale smaller than the site spacing. For the three bands between 1 and 1000 s, strike directions lie near 15° for one group and around −30° for the other group. These periods yield the preferred strike of the bulk of the crust and are dominated by the response of regional large-scale structures. On the basis of strike classification the sites were assigned to one of five sets, each exhibiting similar strikes (Figure 2). Profiles I, II, and V have a best-fitbest fit geoelectric strike of −30° (N30°W), and profiles III and IV have a strike of +15° (N15°E).

Figure 5 shows the RMS error for each of the profiles between the data (impedance tensor components) and the GB distortion decomposition models. The errors of the impedance tensor are assumed to be a minimum of 5%, and a RMS error below 1 indicates that the data fit the distortion model to within 10% in apparent resistivity and 2.8° in phases. Large errors indicate that the data do not fit the model and are due either to 3-D inductive effects of regional structures or to inappropriately small error estimates. Most of the large misfit is concentrated at periods around 1 s, and *Chave and Jones* [1997] have demonstrated that the parametric error estimators used lead to inaccurately small estimates of error at periods of 0.1–10 s. These small values are principally due to division by the square root of the number of estimates, with the implicit assumption that each estimate contributes independently to the average. In the band 0.1–10 s, there are a large number of estimates and correspondingly small estimates of error. In the analyses of *Chave and Jones* [1997], parametric error estimates were compared against nonparametric jackknife ones, and the former were found to be consistently too small at periods of 0.1–10 s by factors of 2–5. Applying such factors to the RMS values depicted in Figure 5 in that period band would reduce most of them to acceptable values.

Support of clockwise rotation of southern Omineca and Intermontane Belts after the mid-Cretaceous and before the Eocene extension comes from paleomagnetic data and from palinspastic reconstruction of the foreland belt [*Sears*, 1994; *Cook*, 1995]. Estimates of rotation from paleomagnetic data indicate large variability from site to site between 60° clockwise to 14° counterclockwise. Palinspastic reconstructions give a clockwise rotation between 25° and 60° depending on the amount of displacement considered [*Cook*, 1995]. The variation of the regional electromagnetic strike (−30°, profiles I, II, and V, and +15° profiles III and IV) may be interpreted to imply a local clockwise rotation of southern Omineca and Intermontane Belts of ∼45°, a value within the bounds given by the other methods.

Once the appropriate strike directions were determined, the data from each site were fit to a frequency-independent distortion model with an assumed strike angle to determine the scaled regional 2-D impedances. Most of the amplitude scaling effects, or static shifts [see, e.g., *Jones*, 1988], were removed by fitting a distortion model and by coalescing the high-frequency asymptotes of the apparent resistivity curves of the two modes to their geometric mean. The remaining shift effect, called site gain by

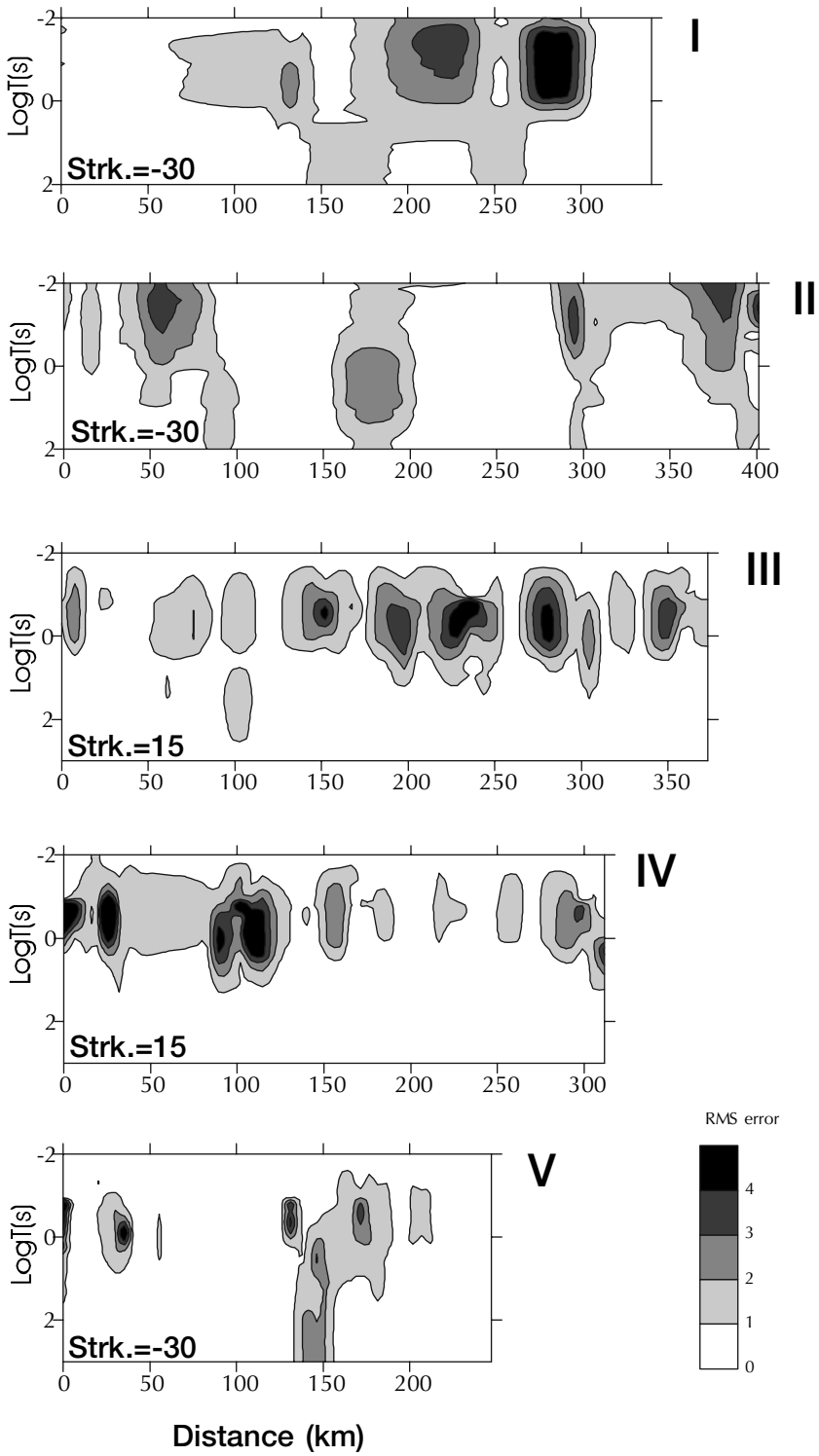

Figure 5. RMS error of misfit between the data (impedance tensor components) and the Groom and Bailey decomposition models for the five profiles. Along each profile the geoelectric strike direction is constant at each frequency and for each site.

Groom and Bailey [1989], was shown by them to be typically small (<1/3 decade) and was accounted for as part of the inversion procedure (see section 5).

5. Two-Dimensional Inversion and Interpretation

For each profile, simultaneous 2-D inversions of the distortion-corrected TE and TM apparent resistivity and phase data were undertaken using the rapid relaxation inversion (RRI) code of *Smith and Booker* [1991]. The final scaling of the apparent resistivities was determined as part of the inversion procedure [*Wu et al.*, 1993]. Neither structural features nor resistivity discontinuities were imposed during the inversion. The RRI inversion approach follows that pioneered by *Constable et al.* [1987] and *DeGroot-Hedlin and Constable* [1990] and determines the resistivity model with least structure most consistent with the data. One must trade off misfit against model smoothness, and we adopted a value of RMS of 5% higher than the minimum reasonable achievable for the impedance tensor components. The resulting regional models are shown in Plate 1, and the model responses fit the apparent resistivity data to within 10% and the phases to within 2.8°, on average. Comparisons between the data and model responses are shown in Plate 2 for the phases from all sites and in Figure 6 for the apparent resistivities for selected key sites in the Intermontane and Omineca Belts. The TM phases at sites located in the westernmost part of profile V for periods longer than 8 s present some problems that have been discussed previously [*Jones et al.*, 1993]. These phases were not used during the 2-D inversion.

The first-order regional results from our MT models are (1) the characterization of the lower crust as a conductive region in comparison with the upper crust in profiles III, IV, and V and (2) the variation of the electrical properties at lower crustal depths along strike in the Omineca Belt. The first result attests to the pervasive nature of the reduced lower crustal resistivity, whereas the second result indicates that the resistivity is likely controlled by tectonic factors.

The general major features in all models from the five profiles are similar, which suggests that the inductive scale length is smaller than the geological horizontal scale length and that the data can be inverted in a 2-D manner to obtain the broad regional pattern of resistivity structure. The regional features from west to east are as follows:

1. The Fraser Fault (FF) separates the Coast Belt from the Intermontane Belt and is imaged by profiles I, III, and IV as an increase in middle-lower crustal resistivity from the Coast Belt to the Intermontane Belt. This is consistent with the model of *Jones et al.* [1992b], although they used a different data set from a short profile that focused on the detail of the FF rather than on regional structures.

2. The Intermontane Belt has a resistive upper crust and a lower crust with resistivity between 100 and 300 Ω m. There is little evident variation in resistivity along strike.

3. The geologically mapped boundary between the southern Intermontane Belt (IB) and Omineca Belt (OB) is the Okanagan Valley Fault (OVF). This boundary was studied in detail by *Marquis et al.* [1995], and their resistivity models, obtained from the MT data along profiles III and IV, show a significant decrease in electrical resistivity at depths of ~10 km across the OVF. This agrees with our models, and, again, differences in detail can be explained by the more focused nature of *Marquis et al.*'s [1995] modeling compared to our own regional approach.

4. To the north, the boundary between the IB and OB is imaged at upper and middle crustal depths as an increase in OB resistivity. In the upper crust of the Omineca Belt along profile I some shallow conductive structures are present, consistent with previous 1-D inversions of the data by *Gough and Majorowicz* [1992]. The bedrock geology, as expressed by the geological map of this region [*Wheeler et al.*, 1991], does not show any exposed potentially conducting units, precluding a ready explanation for the shallow conducting anomalies. Because of the screening effect of the shallow conductive structures in the western OB on profile I, it is not possible to resolve structures with lower conductance at deeper crustal depths.

5. The boundary between the resistive upper crust and the more conductive lower crust is shallower in the OB in comparison with the IB.

6. As discussed above, there is significant along-strike variation in lower crustal resistivity for the OB. In the models from the southern profiles (III and IV) the resistivity decreases from the IB to the OB, whereas in the northern models (I and II) the resistivity increases. The causes and implications of this variation along strike in the OB are discussed below.

7. The Slocan Lake Fault (SLF) is part of a series of extensional faults that accommodated crustal thinning in the Eocene (see discussion in section 1). The resistivity model for profile V images this fault down to lower crustal depths separating structures of different conductivities. Our model broadly agrees with the previous 2-D forward modeling of *Jones et al.* [1993] using a smaller data set crossing the SLF. However, the new inversion model for profile V images a dipping resistivity contrast in the middle crust. This result agrees with the fault geometry imaged by the nearly coincident seismic reflection data [*Cook et al.*, 1992] and the wide-angle velocity model of *Zelt and White* [1995].

6. Comparison With Thermal, Rheological, and Seismological Information

Comparisons of the gross regional seismic and electrical interpretations for southern BC are given in Figure 7. Figure 7b is a synthesis figure, based mainly on the southern profile MT models, of the crustal conductive structure from the Coast Belt in the west to the Foreland Belt in the east. Superimposed on Figure 7b are one-dimensional rheological profiles for the Intermontane, western Omineca (wOB) and eastern Omineca belts (eOB), calculated from information given by *Lowe and Ranalli* [1993] and *Marquis et al.* [1995]. Our calculations infer that the brittle-ductile transition occurs at around 12, 10, and 22 km for the IB, wOB, and eOB, respectively. Following *Hyndman and Lewis* [1999], we consider the uncertainties on the temperature estimates to be ~20%, and those uncertainties correspond to a ±4 km margin of error in the determination of the brittle-ductile transition. These are minimum depths for the transition zone given that we used steady state (conductive) equations. As extension ceased at about 45 Ma, this formalism is appropriate for the upper crust above the brittle-ductile transition but probably not in the ductile regime where convective heat transfer by fluid flow in the porous media and by solid stretching likely dominate. These depths, and their spatial association, agree well with the transition between resistive upper crust and conductive lower crust determined by our models. Unfortunately, we cannot extend this comparison to the central Cordillera: there are no heat flow data in the region of profile I for the OB. The few and sparse heat flow data that exist in the OB close to profile II [*Majorowicz et al.*, 1993; *Hyndman and Lewis*, 1995] suggest some along-strike variation in thermal conditions [*Majorowicz et al.*, 1993], but more data are required to confirm this. *Majorowicz et al.* [1993] showed that the top of the lower crustal conductor found by 1-D inversion of MT data in the Canadian Cordillera is consistent with the geothermally modeled depth to the 450°C isotherm, which can be associated with the brittle-ductile transition in the crust. *Lewis et al.* [1992] suggested a correlation between the depth of the lower crustal reflectivity and heat flow for the eastern part of the Lithoprobe Southern Canadian Cordillera Transect. The agreement in the

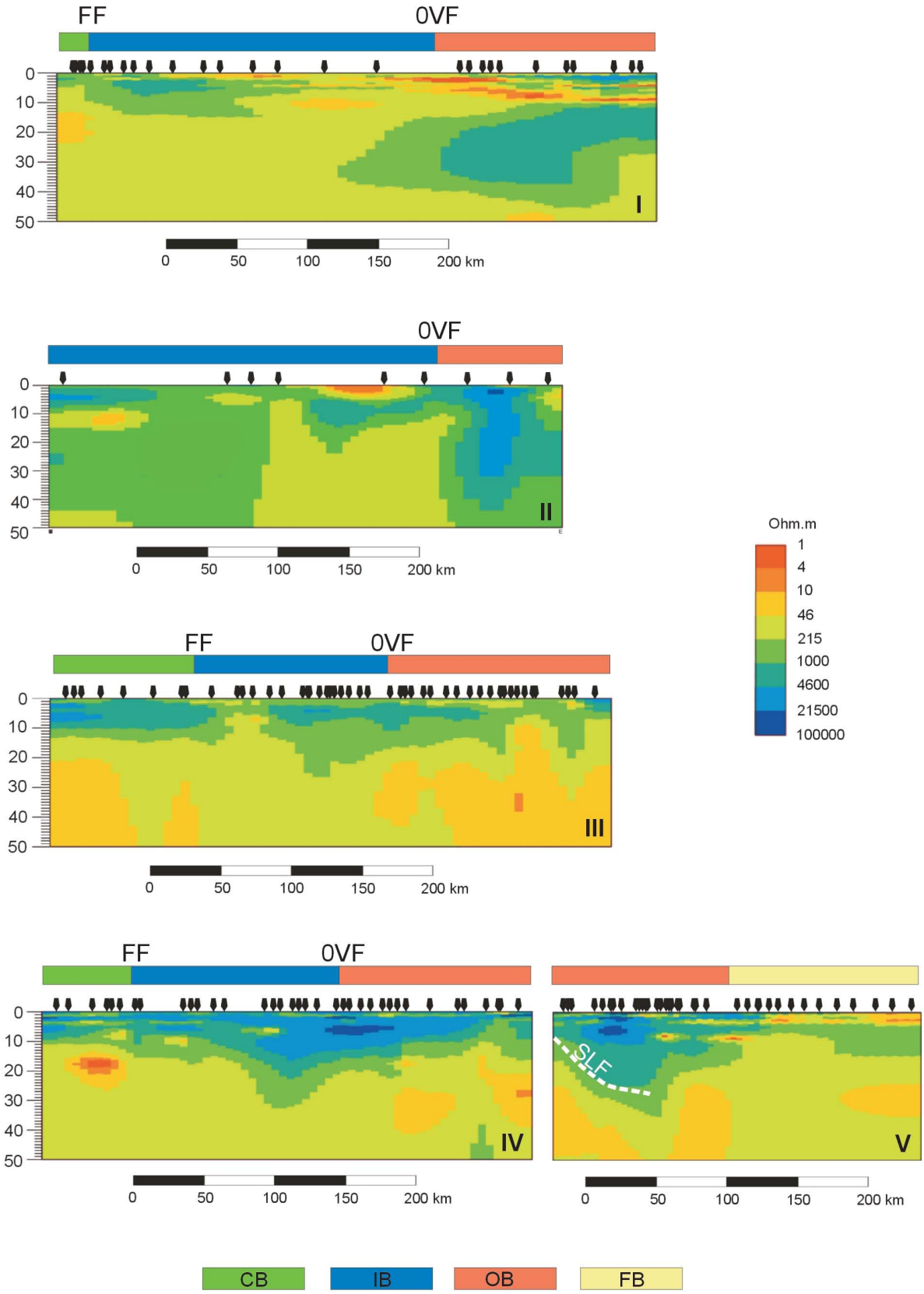

Plate 1. Two-dimensional MT resistivity models obtained by RRI [*Smith and Booker*, 1991; *Wu et al.*, 1993] inversion using both TE and TM mode distortion-decomposed apparent resistivity and phase data. Note vertical exaggeration of 2:1 for all models. CB, Coastal Belt; IB, Intermontane Belt; OB, Omineca Belt; FB, Foreland Belt; FF, Fraser River Fault; OVF, Okanagan Valley Fault; SLF, Slocan Fault.

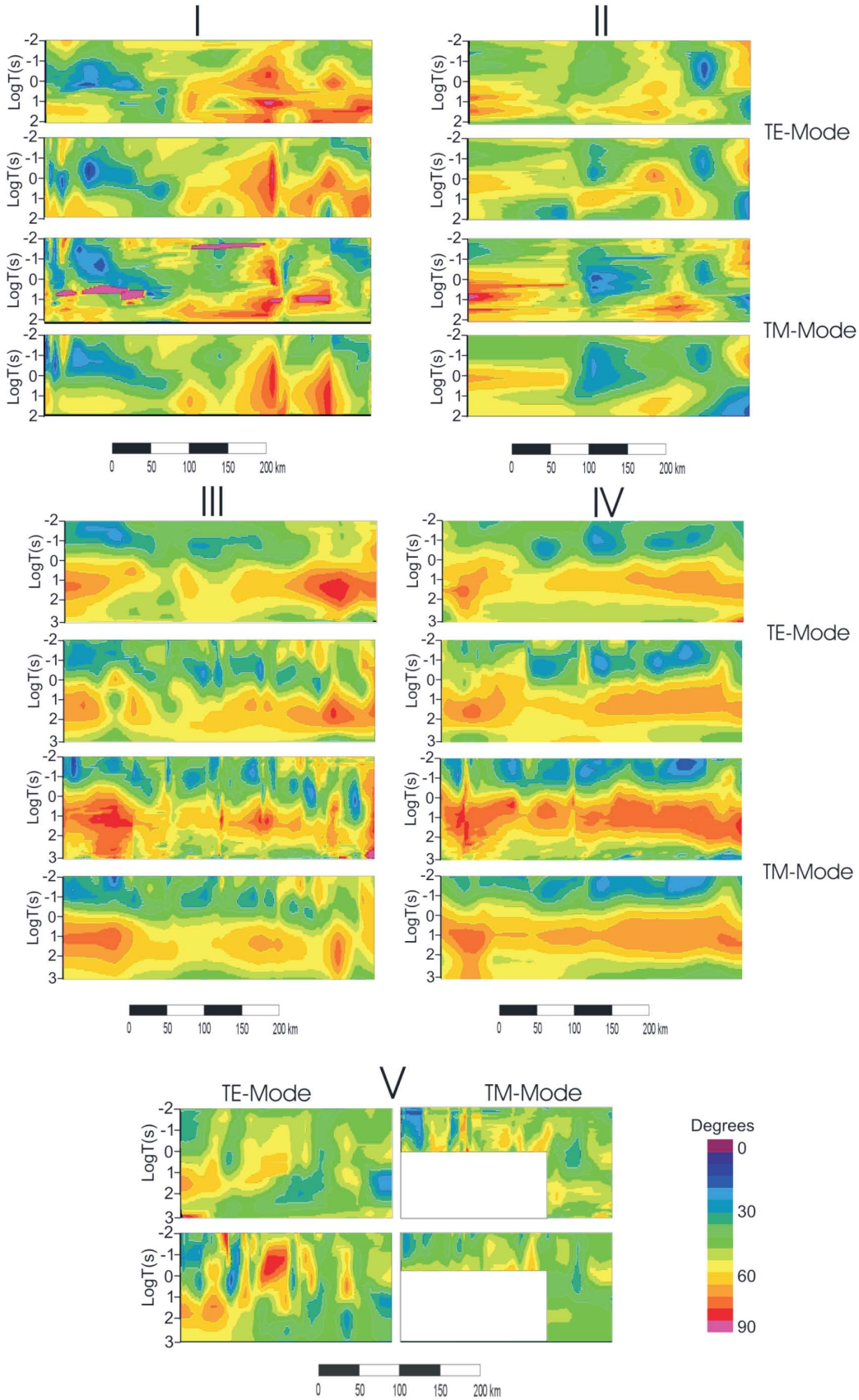

Plate 2. Comparison of phases from both TE and TM mode for the (top) data and (bottom) model responses for each profile.

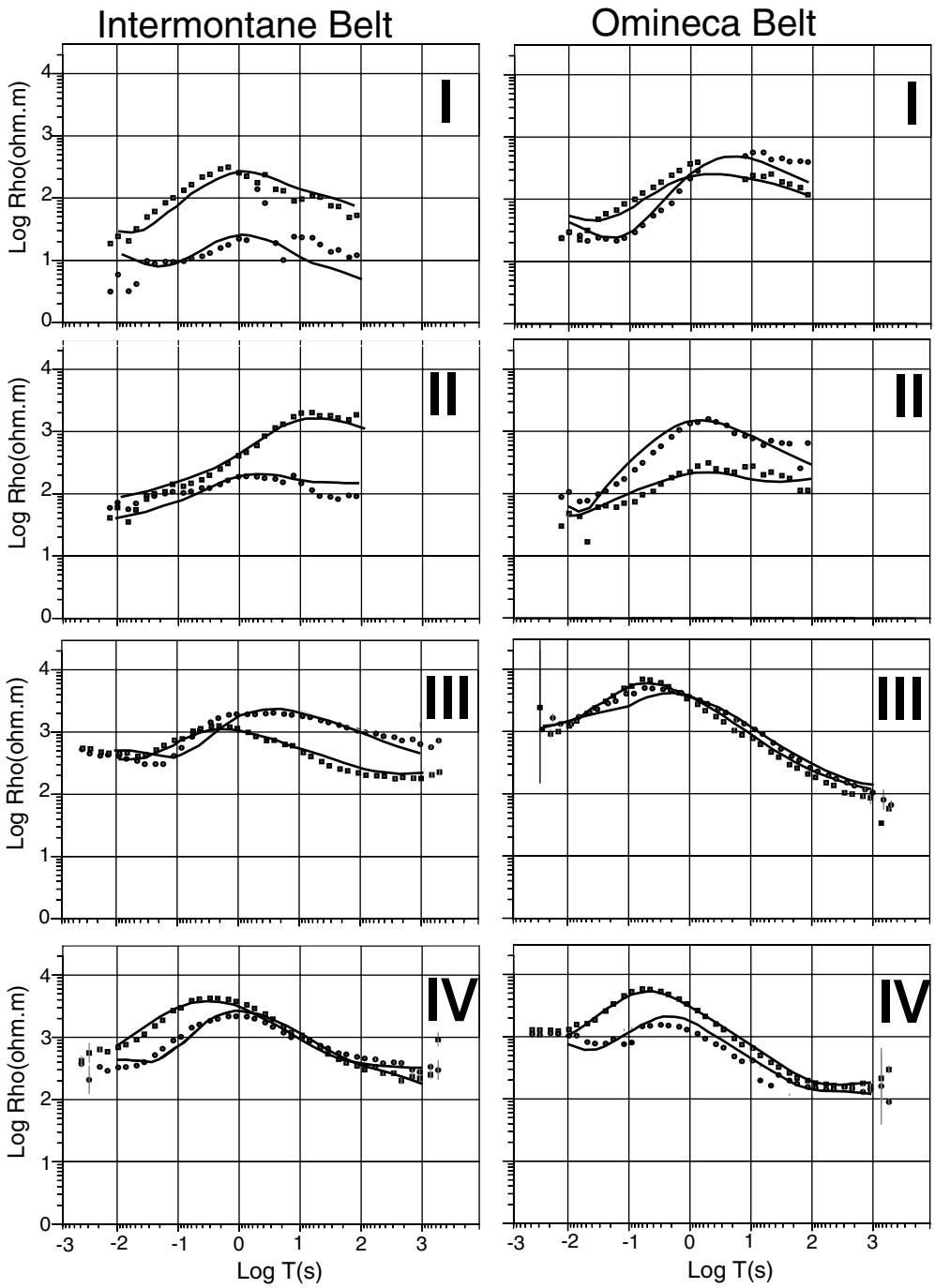

Figure 6. Comparison of apparent resistivities from both modes for the data and model responses at key sites from the Intermontane and Omineca Belts for each of the profiles crossing the belts. Squares, TM mode data; circles, TE mode data. The sites compared are marked in Figure 2 with stars.

brittle-ductile transition depth among these three different physical parameters is consistent with more local and detailed studies undertaken in the Canadian Cordillera [*Marquis et al.*, 1995] and with global compilations [*Jones*, 1987, 1992; *Hyndman and Shearer*, 1989; *Marquis and Hyndman*, 1992], suggesting that a generic physical process due to P-T and fluid conditions is responsible.

From the comparison between the interpreted seismic (Figure 7a) and MT (Figure 7b) interpretations it is clear that the reduced resistivity is located at lower crustal depths and cannot, in general, be associated with a particular geological terrane. On the basis of their different origins it might be expected that different resistivity characteristics would be observed for different terranes, yet our models show instead a belt dependence. Generally, terranes lie exclusively within each of the belts; however, the former are thin upper crustal features, whereas the latter are a consequence of crustal rheology. Such belt dependence, rather than terrane dependence, is also observed in the *P* wave refraction crustal velocity model obtained by *Burianyk and Kanasewich* [1995], where there is not a significant change in the lower crustal velocities across different terranes. There are two likely scenarios possible to explain these observations: (1)

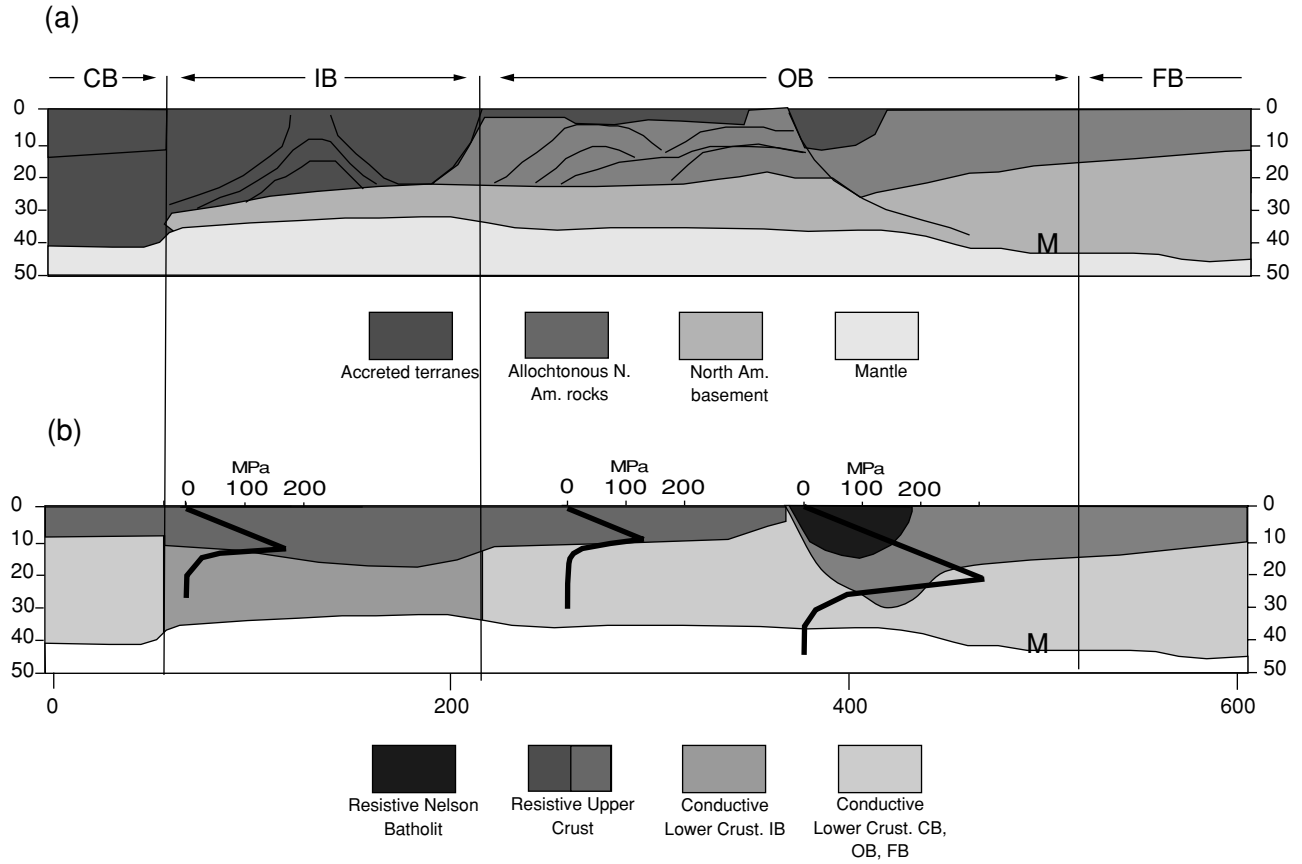

Figure 7. (a) Cartoon of the major seismic features for the southern Canadian Cordillera, redrawn from *Clowes et al.* [1995]. (b) Cartoon of the MT results for the southern Canadian Cordillera based on profiles III, IV and V. The solid lines on the MT cartoon represent the maximum differential stress (in MPa), calculated using standard conductive equations and physical parameters taken from *Lowe and Ranalli* [1993] and *Marquis et al.* [1995]; M is depth of the crust-mantle discontinuity determined by seismic data. Depth and distance are in km.

the terranes are not deeply rooted and we are observing the "original" North America lower crust or (2) postaccretionary physical processes have acted to homogenize the ductile crust within each belt. Interpretation of the seismic reflection data has tended to focus on scenario 1 [*Cook et al.*, 1992], and a similar interpretation is being advocated for the northern Canadian Cordillera [*Cook et al.*, 2001].

7. Physical State of the Lower Crust

The complex interplay between mechanical, chemical, hydrological, and thermal processes in the lower crust makes an analytical approach to their study difficult. Adopting Occam's Razor, the simplest interpretation of the observed spatial correlations is that the variations in electrical, elastic, and rheological properties have a common origin. We recognize the dangers inherent in an apparent correlation of surface data that can belie the true nature of the observed anomalies [*Cook and Jones*, 1995]. However, in this case we are correlating parameters that are likely to be physically related, namely, rheology and resistivity, as both are dramatically affected by the addition of small amounts of water [*Tozer*, 1981]. The identification of a unique mechanism compatible with the physical and chemical state of the lower crust may provide a critically important constraint on the evolution of the geological structures. In this section we will discuss the simplest possible scenarios explaining the predominant features of the derived geophysical models.

From our resistivity models (Plate 1) and the calculation of rheological state from thermal parameters (Figure 6), there appears to be a correlation in depth between the base of the upper crustal resistive layer and the brittle-ductile transition. Below this layer, reduced resistivity at middle and lower crustal depths is most likely a consequence of either electronic conduction in metasediments (graphite or sulphides) or ionic conduction in free fluids, including partial melt [*Jones*, 1992]. Mafic intrusions, horizontal mylonite shear zones, or metamorphic layering, proposed to explain lower crustal reflectivity [*Mooney and Meissner*, 1992], do not decrease electrical resistivity and so can be excluded as candidates to jointly explain the elastic and electrical observations. The presence of interconnected graphite or sulphides can explain the observed resistivity values and has been observed in the upper crust at specific areas in the Purcell Anticlinorium in the eastern part of the southern Canadian Cordillera [*Jones et al.*, 1992a; *Cook and Jones*, 1995; *Gupta and Jones*, 1995]. Even in the case where conditions for the formation of graphite at lower crustal depths were possible, the high dihedral angle of CO_2 fluids and the low diffusivity of graphite [*Watson and Brenan*, 1987] preclude it as a candidate to explain the observed pervasive resistivity. Remobilized vein graphite is a possible candidate. However, a small fraction of either graphite or sulphides will not significantly affect elastic properties [*Marquis and Hyndman*, 1992] and so will not modify the seismic velocity. Partial melt at the boundary between the upper and lower crust (10–15 km) is not possible given that the temperatures [*Hyndman and Lewis*, 1999] are

insufficient to produce partial melting of lower crustal (amphibolite to granulite grade) rocks. However, at the base of the crust the temperature is high enough ($T > 800°C$) to trigger dehydration melting.

One explanation that meets the requirements of low resistivity, reduced crustal strength, and increased seismic reflectivity is the presence of interconnected aqueous fluids in the ductile lower crust. The Canadian Cordillera consists of a region of reworked crust recently accreted from predominantly oceanic and island arc material. In addition, there is a significant source of fluids to be west, namely, the subducting Juan de Fuca plate. The Pb isotopes in the Omineca Belt are also consistent with a deep crustal or mantle hydrothermal fluid [*Beaudoin et al.*, 1991]. Oxygen fugacity data for subduction-zone-related peridotites suggest that the mantle wedge is oxidized relative the oceanic and ancient cratonic mantle [*Parkinson and Arculus*, 1999]. The oxidized nature of the overlying lithosphere in subduction zones may be due to the presence of water and/or melts from the subducted slab [*Parkinson and Arculus*, 1999]. In such a region, ionically conductive fluids are to be expected. Moreover, the presence of fluids will reduce the strength of the lower crust and thus favor the presence of shear zones that can explain the observed reflection seismic pattern [*Marquis et al.*, 1995].

Geophysical experiments on Vancouver Island came to the conclusion that fluids within a shear zone at the 450°C isotherm would explain the observed seismic and electromagnetic behavior [*Jones*, 1987; *Hyndman*, 1988]. Retention of this fluid would be promoted if the vertical permeability of the ductile lower crustal rocks was lowered [*Thompson and Connolly*, 1990], for example, by metamorphic aquitards. A mechanism for generating fluids by metamorphic reactions and its posterior maintenance at lower crustal depths was proposed by *Goldfarb et al.* [1991] to explain isotopic data from Alaska.

8. Variation of Physical Properties Along Strike in the Omineca Belt

A variation in the amount of fluids in the lower crust also offers an explanation for the along-strike resistivity variation of the lower crust in the OB. The southern Omineca Belt underwent short-lived extension in the early Eocene (between 59 and 46 Ma), possibly as a consequence of active mantle upwelling [*Gough*, 1986], passive lithospheric delamination [*Ranalli et al.*, 1989], or gravitational collapse with space accommodation from far-field plate motion, as is the preferred mechanism in the northern Basin and Range [*Sonder and Jones*, 1999]. The crustal response to mantle dynamics was extension and crustal thinning and an increase of crustal temperature and weakening of the crust at shallower depths. At the same time, it likely resulted in high fluid flux from the mantle in the form of CO_2-H_2O brines exsolved from mantle-derived basalts emplaced in the lower crust [*Frost et al.*, 1989]. The migration of the fluids through the crust would have formed mineral systems at higher structural levels in the crust, which is supported by the observed Eocene mineralization in the southern Omineca Belt [*Beaudoin et al.*, 1992]. However, an adequate explanation for fluid retention or recharge must be offered given that extension ceased at ~46 Ma and residency in crust for a uniform temperature of ~600°C for reasonable values of porosity (1%) is short (<1 Myr [*Bailey*, 1990; *Frost and Bucher*, 1994]). One can appeal to a trapping mechanism at the brittle-ductile transition where the fluids concentrate [*Bailey*, 1990], although it would imply the existence of a finite depth conductor. In the southern models the total conductance (thickness-resistivity quotient) of the lower crust is between 500 and 2000 S, with values of electrical resistivity between 10 and 46 Ω m distributed between 15 and 35 km depth. To achieve the same conductance with a 2-km-thick layer, it would be necessary to have resistivity values between 1 and 4 Ω m, and these are too low to be satisfactorily explained by fluids alone. Alternatively, small horizontal compressive stresses can disconnect vertical pores that would otherwise be connected, while retaining horizontal pore interconnection [*Marquis and Hyndman*, 1992]. This mechanism, similar to the one proposed by *Goldfarb et al.* [1991], would explain the maintenance of the fluids during compression due to collision of the Insular terrane subsequent to the Eocene extension event.

Table 1. Variation of Geophysical Parameters Along the Omineca Belt[a]

	Central OB (~52°N)	Southern OB (~49°N)
Heat flow, mW/m^2	100	120
Moho depth, km	33.5	31
Bouguer anomaly, mGal	−50	−120
Lower crust resistivity, Ω m	3000	30
Lower crust *P* wave velocity, km/s	6.5	6.7

[a] Heat flow data from *Majorowicz et al.* [1993]. Depth to the Moho from *Cook* (1995). Bouguer anomaly and lower crust velocity from *Clowes et al.* (1995). Lower crustal resistivity from this work.

Other physical parameters besides electrical resistivity exhibit along-strike variation in the Omineca Belt (Table 1). From north to south, there is an increase in the Bouguer anomaly and an attendant decrease of the depth to the Moho [*Cook et al.*, 1995], an increase of the heat flow [*Majorowicz et al.*, 1993], and an increase of the average lower crustal *P* wave velocity [*Clowes et al.*, 1995] (Table 1). Figure 8 is a cartoon of the N-S crustal conductive structure constructed from the crossing 2-D E-W resistivity models for the Omineca Belt, the position of the lower crust and the low-velocity middle crust determined by seismic refraction, and the crustal thickness [*Kanasewich et al.*, 1994].

Our hypothesis for the presence of fluids should not be seen as a rejection of other mechanisms but as the simplest mechanism that can explain most of the observations. For example, the possible existence of small amounts of partial melting in the lower crust may explain the low resistivity of the southern OB below 25 km depth. The increase of lower crust compressional velocity from north to south in the OB [*Burianyk and Kanasewich*, 1995] could be consistent with mafic underplating, which would have residual melt and would increase the velocity at the same time.

The 3-D magnetotelluric investigation of the California Basin and Range by *Mackie et al.* [1996] revealed a conductive lower crust that they associated with the ongoing extension of this zone. Magnetotelluric studies in the northern Basin and Range subprovince, another region of recent significant extension although far more prolonged, also show an anomalously conductive lower crust [*Wannamaker et al.*, 1997a, 1997b]. Resistivity values are ~8 Ω m below 15–20 km beneath the active eastern Great Basin (EGB) but are higher, ~20 Ω m, below 20–25 km beneath the less active central Great Basin (CGB) to the west. This reduced resistivity is interpreted in terms of interconnected fluids whose composition varies with depth; brines in the upper parts, with depth partitioning of H_2O and CO_2 (discussed by *Jones* [1992]) and partial melting at $T > 800°C$. Such temperatures would be reached close to the Moho (~30–35 km) beneath the CGB but at shallower crustal levels (~25 km) beneath the active EGB. The resistivity contrast between the EGB and CGB is interpreted in terms of differences in physical-chemical states, with the EGB being hotter and containing a higher percentage of fluids compared to the CGB. The source of these fluids is interpreted to result from replenishment through ongoing magmatic underplating.

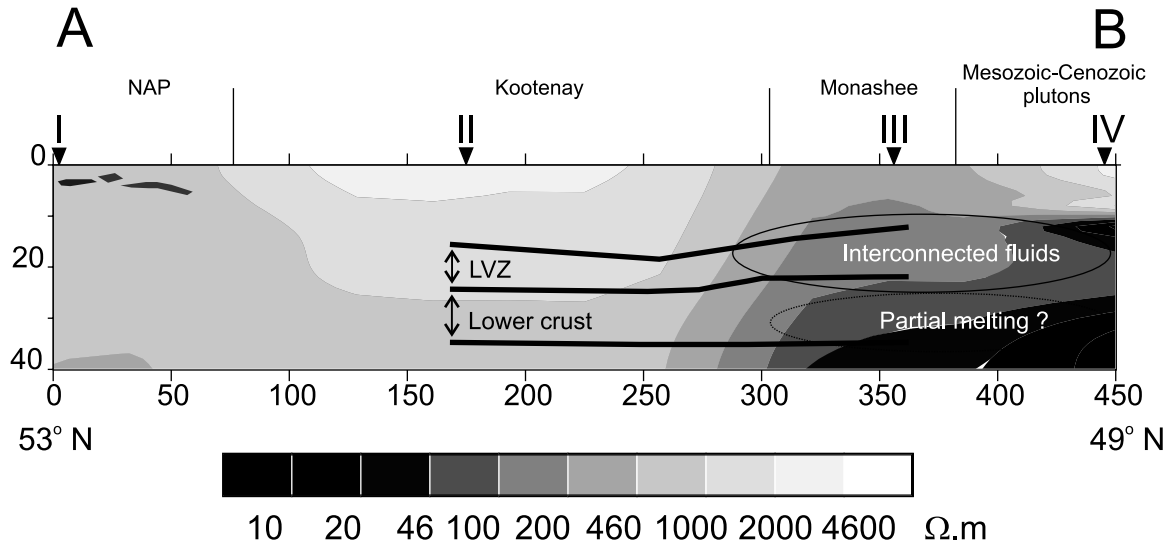

Figure 8. North-south crustal resistivity model of the Omineca Belt constructed from the four 2-D east-west MT models. Seismic layers for the middle and lower crust obtained from *Kanasewich et al.* [1994]. LVZ, low-velocity zone. See Figure 2 for location of the A-B profile.

In our case, the difference in lower crustal resistivity between the central Omineca and southern Omineca is far greater, with values of 1000–4600 Ω m for the former compared to 10–46 Ω m for the latter. The fluid porosity of the lower crust can be estimated from the fluid resistivity and a model of pore fluid connectivity. Given that no data exist from which we can estimate the salinity of the fluids present in the lower crust of the southern Omineca Belt, we consider fluid salinity between 1 and 25 wt %. These values correspond to electrical resitivities of 5 and 0.01 Ω m, respectively [*Nesbitt*, 1993]. For the geometric description of interconnectivity we employ the modified brick layer (MBL) model of *Schilling et al.* [1997]. With these values and MBL model the observed electrical resistivity of the southern Omineca lower crust could be explained with a fluid content of between 0.5% (high salinity) and 10% (low salinity). The southern Omineca can be interpreted in a manner analogous to the Basin and Range in terms of interconnected aqueous brines in the middle crust and upper part of the lower crust and then partial melt below ~25 km. Our interpretation is therefore that the fluid content of the southern Omineca was enhanced by the Eocene extension event. Given the temperature profile for the Omineca, this fluid content will increase the amount of water-undersaturated partial melting below 25 km depth. The central Omineca lower crust is interpreted to be virtually fluid absent (at least of interconnected fluid), as the observed resistivities can be explained by dry candidate lower crustal rocks at those P-T conditions [*Olhoeft*, 1981; *Shankland and Ander*, 1983].

9. Conclusions

Analysis of MT data from over 150 sites in southern and central British Columbia using modern MT tensor decomposition demonstrates that the data from the five profiles can be grouped into two sets each with a distinctive dominant crustal geoelectric strike direction. These strike directions are consistent with a block rotation of the SE part of the Cordillera discussed by *Cook* [1995]. The regional responses in the appropriate strike direction were derived for each of the five sets and were subsequently modeled. The five models generally exhibit similar behavior, with a resistive upper crust overlying a conductive lower crust. The transition between the upper and middle/lower crust is consistent with estimates of the depth to the brittle-ductile transition based on steady state thermal calculations, and a trapped interconnected saline fluid is the likely candidate to explain most of the observed lower crustal resistivity and other geophysical observations.

By far the most important result from this reexamination of the data using consistent analyses and modeling procedures is an identification of a significant variation in the lower crustal resistivity of the Omineca Belt along strike, whereas in contrast, in the neighboring Intermontane Belt, lower crustal resistivity is surprisingly uniform. The central Omineca Belt exhibits a resistive lower crust consistent with candidate rock assemblages at its P-T conditions (1000–4600 Ω m), whereas the lowermost crust (>25 km) of the southern Omineca Belt is 2 orders of magnitude more conducting (10–46 Ω m). We associate this difference with the short-lived extension during the Eocene experienced by the southern Omineca, whereas the central Omineca remained unextended. Our interpretation is that as a consequence of extension, fluids were introduced into the crust by magmatic underplating flux from the mantle. Subsequently, the geothermal profile is sufficient to cause fluid-absent partial melting of the southern Omineca lowermost crust (>25 km). The geothermal profile of the Intermontane Belt is less, based on the observed lower heat flow, such that partial melt is not initiated.

Acknowledgments. The authors acknowledge constructive comments on an earlier version of this paper by Don White and Jim Craven and the reviews of the submitted and revised manuscript by Associate Editor Kathy Whaler, Oliver Ritter, and specially the comments and discussions with Phil Wannamaker. Discussion with our colleagues, especially Rob Berman, Sharon Carr, Don Francis, and Roy Hyndman, aided us in our interpretation. Geological Survey of Canada contribution 2000082. Lithoprobe publication 1236.

References

Bailey, R. C., Trapping of aqueous fluids in the deep crust, *Geophys. Res. Lett.*, *17*, 1129–1132, 1990.

Bardoux, M., and J. C. Mareschal, Extension in south-central British Columbia: Mechanical and thermal controls, *Tectonophysics*, *238*, 451–470, 1994.

Beaudoin, G., B. E. Taylor, and D. F. Sangster, Silver-lead-zinc veins, metamorphic core complexes, and hydrologic regimes during crustal extension, *Geology*, *19*, 1217–1220, 1991.

Beaudoin, G., J. C. Roddick, and D. F. Sangster, Eocene age for Ag-Pb-Zn-Au vein and replacement deposits of Kokanee Range, British Columbia, *Can. J. Earth Sci.*, *29*, 3–14, 1992.

Brown, R. L., and J. M. Journeay, Tectonic denudation of the Shuswap metamorphic terrane of southeastern British Columbia, *Geology*, *15*, 142–146, 1987.

Burianyk, M. J. A., and E. R. Kanasewich, Crustal velocity structure of the Omineca and Intermontane Belts, southeastern Canadian Cordillera, *J. Geophys. Res.*, *100*, 15,303–15,316, 1995.

Carr, S. D., and D. L. Parkinson, Eocene stratigraphy, age of the Coryell batholith, and extensional faults in the Granby Valley, southern British Columbia, in *Current Research, Part E, Pap. Geol. Surv. Can.*, *89-1E*, 79–87, 1989.

Chave, A. D., and A. G. Jones, Electric and magnetic field distortion decomposition of BC87 data, *J. Geomagn. Geoelectr.*, *49*, 767–789, 1997.

Clowes, R. M., M. T. Brandon, A. G. Green, C. J. Yorath, A. Sutherland Brown, E. R. Kanasewich, and C. Spencer, Lithoprobe-Southern Vancouver Island: Cenozoic subduction complex imaged by deep seismic reflections, *Can. J. Earth Sci.*, *24*, 31–51, 1987.

Clowes, R. M., F. A. Cook, A. G. Green, C. E. Keen, J. N. Ludden, J. A. Percival, G. M. Quinlan, and G. F. West, Lithoprobe: New perspective on crustal evolution, *Can. J. Earth Sci.*, *29*, 1813–1864, 1992.

Clowes, R. M., C. A. Zelt, J. R. Amor, and R. M. Ellis, Lithospheric structure in the southern Canadian Cordillera from a network of seismic refraction lines, *Can. J. Earth Sci.*, *32*, 1485–1513, 1995.

Coney, P. J., and T. A. Harms, Cordilleran metamorphic core complexes: Cenozoic extensional relics of Mesozoic compression, *Geology*, *12*, 550–554, 1984.

Coney, P. J., P. L. Jones, and J. W. H. Monger, Cordilleran suspect terranes Nature, *288*, 329–333, 1980.

Constable, S. C., R. L. Parker, and C. G. Constable, Occam's inversion: A practical algorithm for generating smooth models from electromagnetic sounding data, *Geophysics*, *52*, 289–300, 1987.

Cook, F. A.,Lithospheric processes and products in the southern Canadian Cordillera: A Lithoprobe perspective, *Can. J. Earth Sci.*, *32*, 1803–1824, 1995.

Cook, F. A., and A. G. Jones, Seismic reflections and electrical conductivity: A case of Holmes' curious dog?, *Geology*, *23*, 141–144, 1995.

Cook, F. A., J. L. Varsek, R. M. Clowes, E. R. Kanasewich, C. S. Spencer, R. R. Parrish, R. L. Brown, S. D. Carr, B. J. Johnson, and R. A. Price, Lithoprobe crustal reflection cross section of the southern Canadian Cordillera, 1, Foreland thrust and fold belt to Fraser River fault, *Tectonics*, *11*, 12–35, 1992.

Cook, F. A., R. M. Clowes, D. B. Snyder, A. J. van der Verden, K. W. Hall, P. Erdmer, and C. Evenchick, Lithoprobe seismic reflection profiling of the northern Canadian Cordillera: First results of the SNORCLE profiles 2 and 3, in *SNORCLE Transect and Cordilleran Tectonics Workshop Meeting*, compiled by F. Cook and P. Erdmer, *Lithoprobe Rep. 79*, pp. 36–49, Lithoprobe Secretariat, Univ. of British Columbia, Vancouver, British Columbia, Canada, 2001.

DeGroot-Hedlin, C., and S. C. Constable, Occam's inversion to generate smooth two-dimensional models from magnetotelluric data, *J. Geomagn. Geoelectr.*, *55*, 1613–1624, 1990.

Duba, A., S. Heikamp, W. Meurer, G. Nover, and G. Will, Evidence from borehole samples for the role of accessory minerals in lower-crustal conductivity, *Nature*, *367*, 59–61, 1994.

ELEKTB Group, KTB and the electrical conductivity of the crust, *J. Geophys. Res.*, *102*, 18,289–18,305, 1997.

Engebretson, D. C., A. Cox, and R. G. Gordon, Relative motions between oceanic plates of the Pacific Basin, *J. Geophys. Res.*, *89*, 10,291–10,310, 1984.

Frape, S. K., and P. Fritz, Water-rock interaction and chemistry of groundwaters from the Canadian Shield, *Geochim. Cosmochim. Acta*, *48*, 1617–1627, 1984.

Frost, B. R., and K. Bucher, Is water responsible for geophysical anomalies in the deep continental crust?-A petrological perspective, *Tectonophysics*, *231*, 293–309, 1994.

Frost, B. R., C. Frost, and J. L. R. Touret, Magmas as a source of heat and fluids in granulite metamorphism, in *Fluid Movements-Element Transport and the Composition of the Deep Crust, NATO ASI Ser., Ser. C*, vol. 281, edited by D. Bridgewater, pp. 1–18, Kluwer Acad., Norwell, Mass., 1989.

Gabrielse, H., and C. J. Yorath, Introduction, in *The Geology of North America*, vol. G-2, *Geology of the Cordilleran Orogen in Canada*, edited by H. Gabrielse and C. J. Yorath, pp. 15–59, Geol. Soc. of Am., Boulder, Colo., 1991.

Goldfarb, R. J., L. W. Snee, L. D. Miller, and R. J. Newberry, Rapid dewatering of the crust deduced from ages of mesothermal gold deposits, *Nature*, 296–298, 1991.

Gough, D. I., Mantle upflow tectonics and the Canadian Cordillera, *J. Geophys. Res.*, *91*, 1909–1919, 1986.

Gough, D. I., and J. A. Majorowicz, Magnetotelluric soundings, structure, and fluids in the southern Canadian Cordillera, *Can. J. Earth Sci.*, *29*, 609–620, 1992.

Groom, R. W., and R. C. Bailey, Decomposition of magnetotelluric impedance tensors in the presence of local three-dimensional galvanic distortion, *J. Geophys. Res.*, *94*, 1913–1925, 1989.

Groom, R. W., R. D. Kurtz, A. G. Jones, and D. E. Boerner, A quantitative methodology for determining the dimensionality of conductivity structure and the extraction of regional impedance responses from magnetotelluric data, *Geophys. J. Int.*, *115*, 1095–1118, 1993.

Gupta, J. C., and A. G. Jones, Electrical conductivity structure of the Purcell Anticlinorium in southeast British Columbia and northwest Montana, *Can. J. Earth Sci.*, *32*, 1563–1583, 1995.

Hyndman, R. D., Dipping seismic reflectors, electrically conductive zones, and trapped water in the crust over a subducting plate, *J. Geophys. Res.*, *93*, 13,391–13,405, 1988.

Hyndman, R. D., and T. J. Lewis, Review of the thermal regime along the southern Canadian Cordillera Lithoprobe corridor, *Can. J. Earth Sci.*, *32*, 1611–1617, 1995.

Hyndman, R. D., and T. J. Lewis, Geophysical consequences of the cordillera-craton thermal transition in southwestern Canada, *Tectonophysics*, *306*, 397–422, 1999.

Hyndman, R. D., and P. M. Shearer, Water in the lower continental crust: Modelling magnetotelluric and seismic reflection results, *Geophys. J. Int.*, *98*, 343–365, 1989.

Jones, A. G., MT and reflection: An essential combination, *Geophys. J. R. Astron. Soc.*, *89*, 7–18, 1987.

Jones, A. G., Static shift of magnetotelluric data and its removal in a sedimentary basin environment, *Geophysics*, *53*, 967–978, 1988.

Jones, A. G., Electrical conductivity of the continental lower crust, in *Continental Lower Crust*, edited by D. M. Fountain, R. J. Arculus, and R. W. Kay, pp. 81–143, Elsevier Sci., New York, 1992.

Jones, A. G., Electromagnetic images of modern and ancient subduction zones, *Tectonophysics*, *219*, 29–45, 1993.

Jones, A. G., and I. Dumas, Electromagnetic images of a volcanic zone, *Phys. Earth Planet. Inter.*, *81*, 289–314, 1993.

Jones, A. G., and D. I. Gough, Electromagnetic images of crustal structures in southern and central Canadian Cordillera, *Can. J. Earth Sci.*, *32*, 1541–1563, 1995.

Jones, A. G., and R. W. Groom, Strike angle determination from the magnetotelluric tensor in the presence of noise and local distortion: Rotate at your peril!, *Geophys. J. Int.*, *113*, 524–534, 1993.

Jones, A. G., D. I. Gough, R. D. Kurtz, J. M. DeLaurier, D. E. Boerner, J. A. Craven, R. G. Ellis, and G. W. McNeice, Electromagnetic images of regional structure in the southern Canadian Cordillera, *Geophys. Res. Lett.*, *12*, 2373–2376, 1992a.

Jones, A. G., R. D. Kurtz, D. E. Boerner, J. A. Craven, G. W. McNeice, D. I. Gough, J. M. DeLaurier, and R. G. Ellis, Electromagnetic images of the Fraser River Fault system, *Geology*, *20*, 561–564, 1992b.

Jones, A. G., R. W. Groom, and R. D. Kurtz, Decomposition and modelling of the BC87 dataset, *J. Geomagn. Geoelectr.*, *45*, 1127–1150, 1993.

Jones, A. G., T. J. Katsube, and P. Schwann, The longest conductivity anomaly in the world explained: Sulphides in fold hinges causing very high electrical anisotropy, *J. Geomagn. Geoelectr.*, *49*, 1619–1629, 1997.

Kanasewich, E. R., M. J. A. Burianyk, R. M. Ellis, R. M. Clowes, D. J. White, T. Cote, D. A. Forsyth, J. H. Luetgert, and G. D. Spence, Crustal velocity structure of the Omineca Belt, southeastern Canadian Cordillera, *J. Geophys. Res.*, *99*, 2653–2670, 1994.

Kurtz, R. D., J. M. DeLaurier, and J. C. Gupta, The electrical conductivity distribution beneath Vancouver Island: A region of active plate subduction, *J. Geophys. Res.*, *95*, 10,929–10,946, 1990.

Ledo, J. J., C. Ayala, J. Pous, P. Queralt, A. Marcuello, and J. A. Muñoz, New geophysical constraints on the deep structure of the Pyrenees, *Geophys. Res. Lett.*, *27*, 1037–1040, 2000.

Lewis, T. J., W. H. Bentkowski, and R. D. Hyndman, Crustal temperatures near the Lithoprobe Southern Canadian Cordillera Transect, *Can. J. Earth Sci.*, *29*, 1124–1197, 1992.

Lowe, C., and G. Ranalli, Density, temperature, and rheological models for the southeastern Canadian Cordillera: Implications for its geodynamic evolution, *Can. J. Earth Sci.*, *30*, 77–93, 1993.

Mackie, R. L., T. R. Madden, and S. K. Park, A three-dimensional magnetotelluric investigation of the California Basin and Range, *J. Geophys. Res.*, *101*, 16,221–16,239, 1996.

Majorowicz, J. A., and D. I. Gough, Crustal structures from MT soundings in the Canadian Cordillera, *Earth Planet. Sci. Lett.*, *102*, 444–454, 1991.

Majorowicz, J. A., and D. I. Gough, A model of crustal conductive structure in the Canadian Cordillera, *Geophys. J. Int.*, *117*, 301–312, 1994.

Majorowicz, J. A., D. I. Gough, and T. J. Lewis, Correlation between the depth to the lower crustal high conductive layer and heat flow in the Canadian Cordillera, *Tectonophysics*, *225*, 49–56, 1993.

Mareschal, J.-C., Thermal regime and post-orogenic extension in collision belts, *Tectonophysics*, *238*, 471–484, 1994.

Marquis, G., and R. D. Hyndman, Geophysical support for aqueous fluids in the deep crust: Seismic and electrical relationships, *Geophys. J. Int.*, *110*, 91–105, 1992.

Marquis, G., A. G. Jones, and R. D. Hyndman, Coincident conductive and reflective middle and lower crust in southern British Columbia, *Geophys. J. Int.*, *120*, 111–131, 1995.

McNeice, G., and A. G. Jones, Multi-site, multi-frequency tensor decomposition of magnetotelluric data, *Geophysics*, *66*, 158–173, 2001.

Monger, J. W. H., Canadian Cordilleran tectonics: From geosynclines to crustal collage, *Can. J. Earth Sci.*, *30*, 209–231, 1993.

Monger, J. W. H., P. van der Heyden, J. M. Journey, C. A. Evenchick, and J. B. Mahoney, Jurassic-Cretaceous basins along the Canadian Coast Belt: Their bearing on pre-mid-Cretaceous sinistral displacements, *Geology*, *22*, 175–178, 1994.

Mooney, W. D., and R. Meissner, Multi-genetic origin of crustal reflectivity: A review of seismic reflection profiling of the continental lower crust and Moho, in *Continental Lower Crust*, edited by D. M. Fountain, R. Arculus, and R. W. Kay, pp. 45–71, Elsevier Sci., New York, 1992.

Nesbitt, B.E., Electrical resistivities of crustal fluids, *J. Geophys. Res.*, *98*, 4301–4310, 1993.

Nesbitt, B. E., and K. Muehlenbachs, Stable isotopic constraints on the nature of the syntectonic fluid regime of the Canadian Cordillera, *Geophys. Res. Lett.*, *18*, 963–966, 1991.

Nesbitt, B. E., and K. Muehlenbachs, Geochemistry of syntectonic, crustal fluid regimes along the Lithoprobe Southern Canadian Cordillera Trancset, *Can. J. Earth Sci.*, *32*, 1699–1719, 1995.

Olhoeft, G. R., Electrical properties of granite with implications for the lower crust, *J. Geophys. Res.*, *86*, 931–936, 1981.

Parkinson, I. J., and R. J. Arculus, The redox state of subduction zones: Insights from arc-peridotites, *Chem. Geol.*, *160*, 409–423, 1999.

Parrish, R. R., S. D. Carr, and D. L. Parkinson, Eocene extensional tectonics and geochronology of the southern Omineca Belt, British Columbia and Washington, *Tectonics*, *7*, 181–212, 1988.

Partzsch, G. M., F. R. Schilling, and J. Arndt, The influence of partial melting on the electrical behavior of crustal rocks: Laboratory examinations, model calculations and geological interpretations, *Tectonophysics*, *317*, 189–203, 2000.

Ranalli, G., R. L. Brown, and R. Bosdachin, A geodynamic model for extension in the Shuswap core complex, southeastern Canadian Cordillera, *Can. J. Earth Sci.*, *26*, 1647–1653, 1989.

Ritter, P., and O. Ritter, The BC87 dataset: Application of hypothetical event analysis on distorted GDS response functions and some thin sheet modelling studies of the deep crustal conductor, *J. Geomagn. Geoelectr.*, *49*, 757–766, 1997.

Schilling, F. R., G. M. Partzsch, H. Brasse, and G. Schwarz, Partial melting below the magmatic arc in the central Andes deduced from geoelectromagnetic field experiments and laboratory data, *Phys. Earth Planet. Inter.*, *103*, 17–31, 1997.

Sears, J. W., Thrust rotation of the belt basin, Canada and United States, *Northwest Geology*, *23*, 81–92, 1994.

Shankland, T. J., and M. E. Ander, Electrical conductivity, temperatures, and fluids in the lower crust, *J. Geophys. Res.*, *88*, 9475–9484, 1983.

Smith, J. T., and J. R. Booker, Rapid inversion of two and three-dimensional magnetotelluric data, *J. Geophys. Res.*, *96*, 3905–3922, 1991.

Sonder, L. J., and C. H. Jones, Western United States extension: How the west was widened, *Annu. Rev. Earth Planet. Sci.*, *27*, 417–462, 1999.

Thompson, A. B., Metamorphism and fluids, in *Understanding the Earth*, edited by G. Brown, C. Hawkesworth, and C. Wilson, pp. 222–248, Cambridge Univ. Press, New York, 1992.

Thompson, A. B., and J. A. D. Connolly, Metamorphic fluids and anomalous porosities in the lower crust, *Tectonophysics*, *182*, 47–55, 1990.

Tozer, D. C., The mechanical and electrical properties of Earth's asthenosphere, *Phys. Earth Planet. Inter.*, *25*, 280–296, 1981.

Vozoff, K., The magnetotelluric method, in *Electromagnetic Methods in Applied Geophysics-Applications*, pp. 641–712, Soc. of Explor. Geophys., Tulsa, Okla., 1991.

Wannamaker, P. E., Comment on "The petrologic case for a dry lower crust" by Bruce W.D. Yardley and John W. Valley, *J. Geophys. Res.*, *105*, 6057–6062, 2000.

Wannamaker, P. E., J. R. Booker, A. G. Jones, A. D. Chave, J. H. Filloux, H. S. Waff, and L. K. Law, Resistivity cross section through the Juan de Fuca subduction system and its tectonic implications, *J. Geophys. Res.*, *94*, 14,127–14,144, 1989.

Wannamaker, P. E., W. M. Doerner, J. A. Stodt, and J. M. Johnson, Subdued state of tectonism of the Great Basin interior relative to its eastern margin based on deep resistivity structure, *Earth Planet. Sci. Lett.*, *150*, 41–53, 1997a.

Wannamaker, P. E., J. M. Johnson, J. A. Stodt, and J. R. Booker, Anatomy of the southern Cordilleran hingeline, Utah and Nevada, from deep electrical resistivity profiling, *Geophysics*, *62*, 1069–1086, 1997b.

Watson, E. B., and J. M. Brenan, Fluids in the lithosphere, 1, Experimentally-determined wetting characteristics of CO_2-H_2O fluids and their implications for fluid transport, host-rock physical properties, and fluid inclusion formation, *Earth Planet. Sci. Lett.*, *85*, 497–515, 1987.

Wheeler, J. O., A. J. Brookfield, H. Gabrielse, J. W. Monger, H. W. Tipper, and G. J. Woodsworth, Terrane map of the Canadian Cordillera, *Map 1713A*, Geol. Surv. of Can., Ottawa, 1991.

Wilson, J. T., On the building and classification of mountains, *J. Geophys. Res.*, *95*, 6611–6628, 1991.

Wu, N., J. R. Booker, and J. T. Smith, Rapid two-dimensional inversion of COPROD2 data, *J. Geomagn. Geoelectr.*, *45*, 1073–1087, 1993.

Zelt, C. A., and D. White, Crustal structure of the southeastern Canadian Cordillera from wide-angle seismic data, *J. Geophys. Res.*, *100*, 24,255–24,273, 1995.

A. G. Jones and J. Ledo, Geological Survey of Canada, 615 Booth St., Ottawa, Ontario, Canada, K1A 0E9. (ajones@cg.nrcan.gc.ca; ledo@cg.nrcan.gc.ca)

(Received June 28, 2000; revised December 15, 2000;
accepted July 14, 2001.)